

Electronic Supplementary Material

The micro-sized hydrothermal carbon supporting metal oxide nanoparticles as efficient catalyst for mono-dehydration of sugar alcohol

Contents

1. SEM image of graphene oxide (GO) (Fig. S1)
2. AFM study of synthetic samples (Fig. S2)
3. TEM images of synthetic samples (Fig. S3)
4. The XPS survey scan for synthetic samples (Fig. S4)
5. XPS measurement of C 1s region for synthetic samples (Fig. S5)
6. XPS measurement of O 1s region for synthetic sample (Fig. S6)
7. Low-angle XRD patterns of powdered samples (Fig. S7)
8. Wide-angle XRD patterns of powdered samples with low crystallinity (Fig. S8)
9. XRD comparison of synthetic product with standard component (Fig. S9)
10. Static contact angles of synthetic samples (Fig. S10)
11. Determination of acid amount of solid sample
12. FT-IR spectra of synthetic samples (Fig. S11)
13. Catalytic dehydration of D-sorbitol to fine chemicals in water (Table S1)
14. Catalyst recycling and real-time UV monitoring (Fig. S12)
15. UV-Vis monitoring catalytic solution (Fig. S13)
16. The calculated contour of HOMO and LUMO for transition states TS8-TS11 (Fig. S14)
17. GC-MS examples for Table S1 (Fig. S15-S30)
18. GC-MS examples for Table 3 (Fig. S31-S44)
19. GC-MS examples for Table 4 (Fig. S45-S58)
20. GC-MS examples for Table 5 (Fig. S59-S64)
21. GC-MS examples for recycling (Fig. S65-S70)

Reference

1. SEM image of graphene oxide (GO)

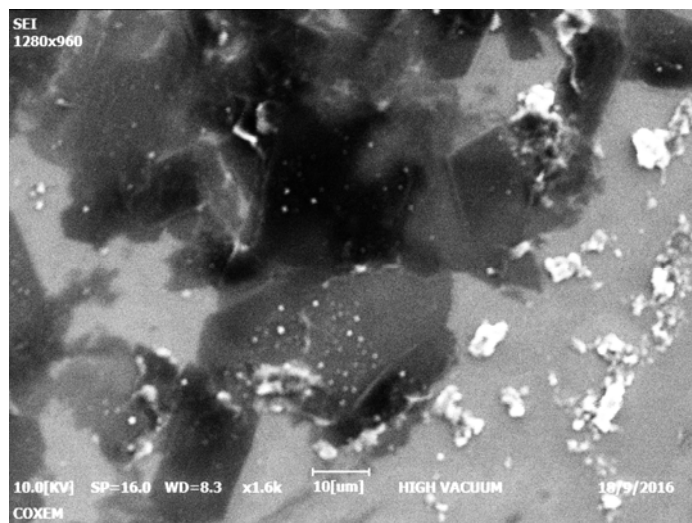


Fig. S1 SEM image of GO.

2. AFM study of synthetic samples

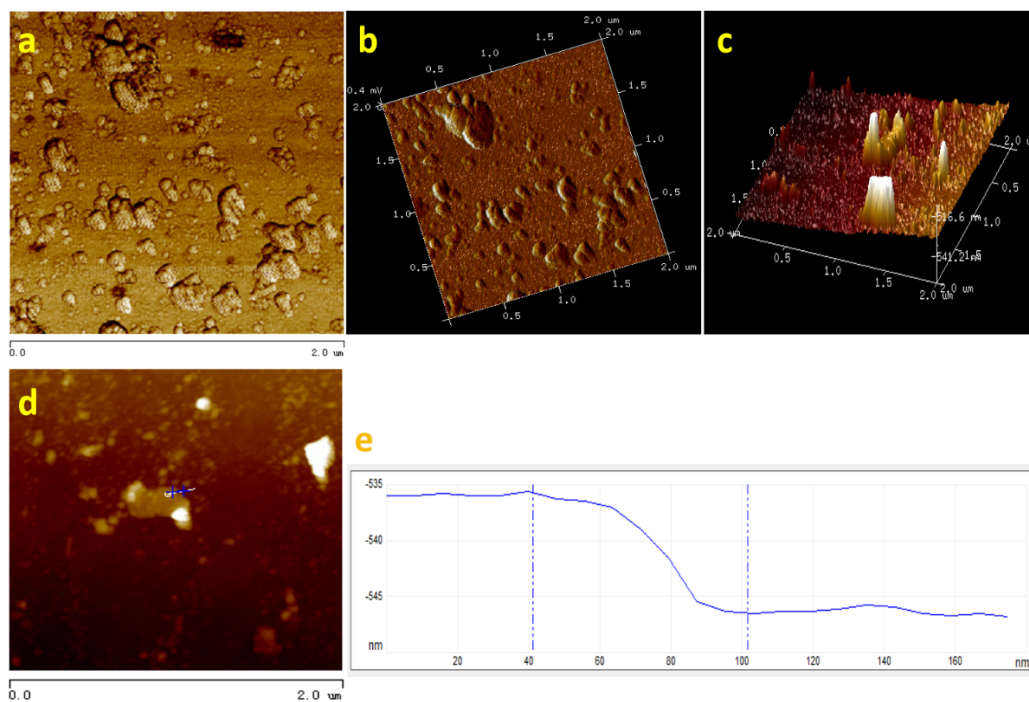


Fig. S2 AFM study of synthetic samples.

(a) AFM two-dimensional models of C3; (b) AFM three-dimensional models of C3; (c) AFM three-dimensional model of C5; (d-e) height measurement of AFM three-dimensional model of C5.

3. TEM images of synthetic sample

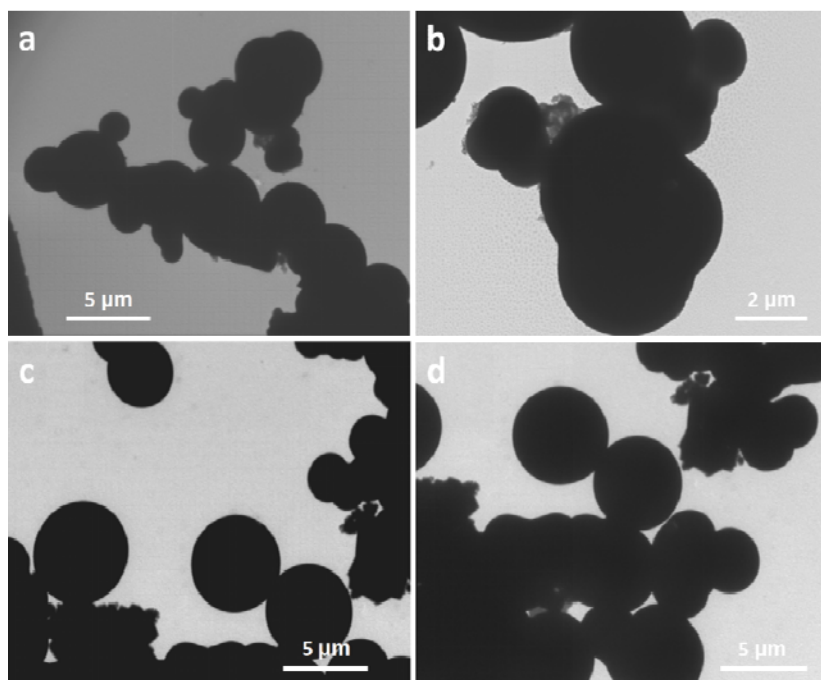


Fig. S3 TEM images of synthetic sample.

(a) C3 (magnification of 6,800×); (b) C3 (14,000×); (c) C4 (6,800×); (d) C4 (6,800×).

4. The XPS survey scan for synthetic samples

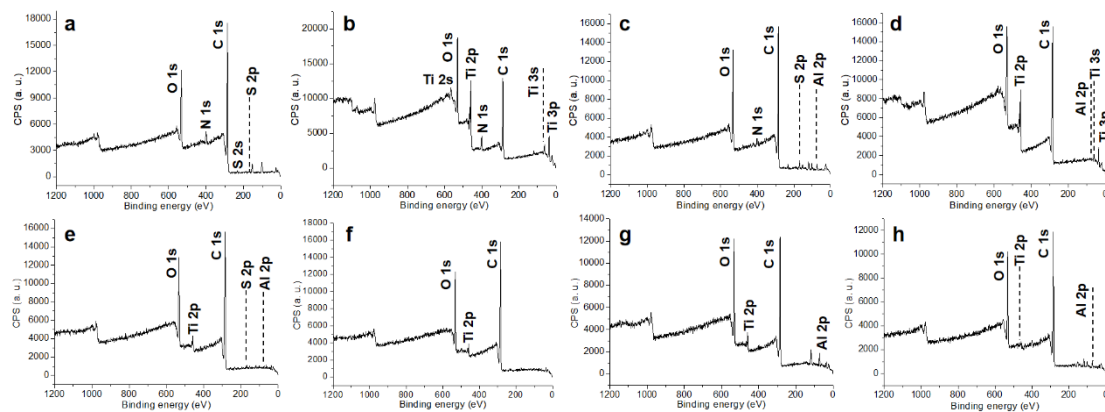


Fig. S4 The XPS survey scan.

(a) C1; (b) C2; (c) C3; (d) C4; (e) C5; (f) C6; (g) C7; (h) C8.

5. XPS measurement of C 1s region for synthetic samples

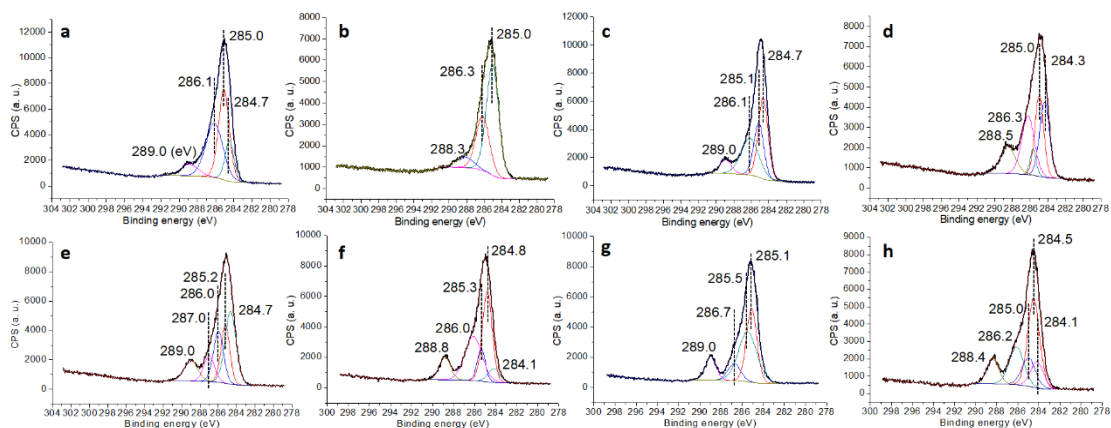


Fig. S5 XPS measurement of C 1s region for synthetic sample.

(a) C1; (b) C2; (c) C3; (d) C4; (e) C5; (f) C6; (g) C7; (h) C8.

6. XPS measurement of O 1s region for synthetic sample

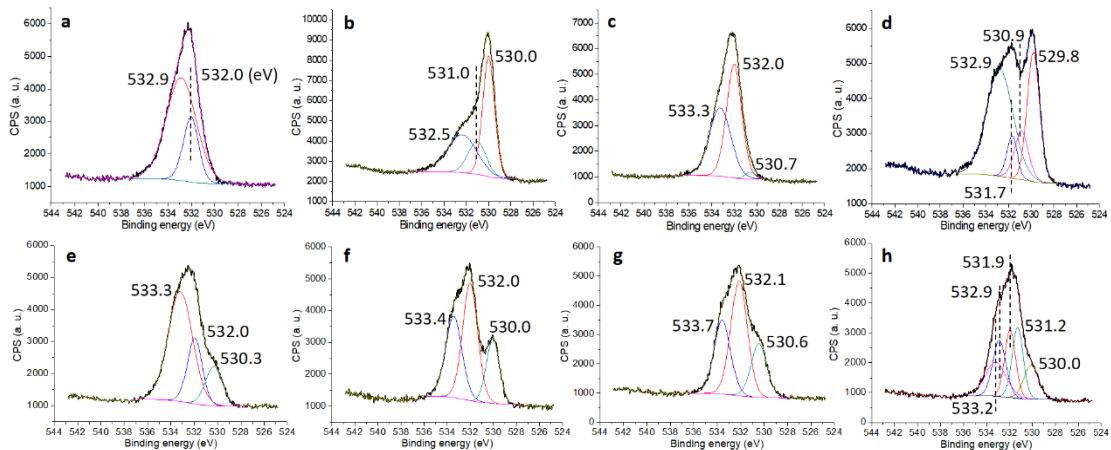


Fig. S6 XPS measurement of O 1s region for synthetic sample.

(a) C1; (b) C2; (c) C3; (d) C4; (e) C5; (f) C6; (g) C7; (h) C8.

7. Low-angle XRD for powdered samples ($2\theta = 0.5^\circ\text{-}10^\circ$)

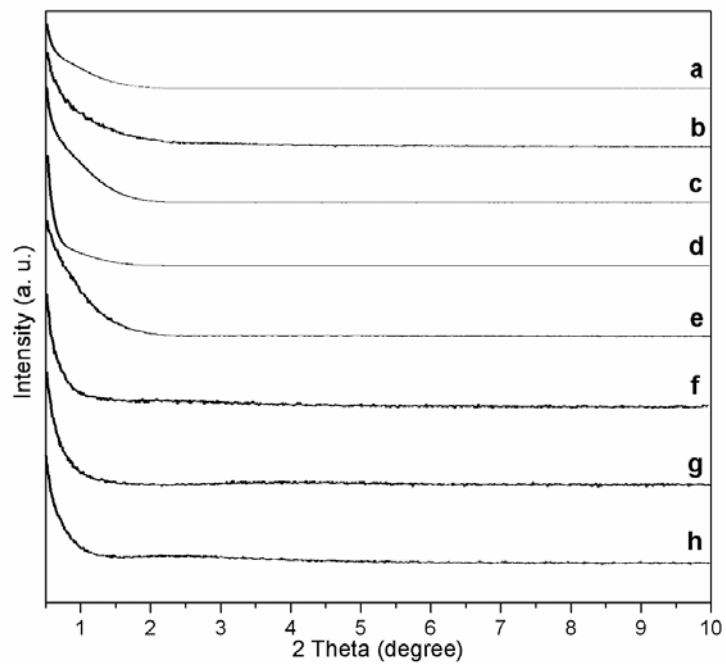


Fig. S7 Low-angle XRD for powdered samples ($2\theta = 0.5^\circ\text{-}10^\circ$).

(a) C1; (b) C2; (c) C3; (d) C4; (e) C5; (f) C6; (g) C7; (h) C8.

8. Wide-angle XRD patterns of powdered samples with low crystallinity

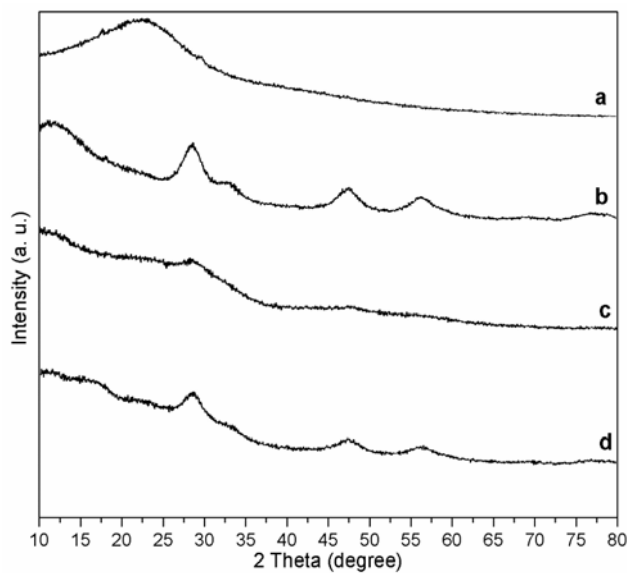


Fig. S8 Wide-angle XRD patterns of powdered samples with low crystallinity.

(a) C1; (b) C6; (c) C7; (d) C8.

Fig. S10 Static contact angles of synthetic samples.

(a) C1; (b) C2; (c) C3; (d) C4; (e) C5; (f) C6; (g) C7; (h) C8.

11. Determination of acid amount of solid sample

The acid amount of solid catalyst is determined by *n*-butylamine titration in association with bromophenol blue sodium salt as indicator [a]. In practice, solid sample (300 mg) and *n*-butylamine (1.25 mmol) are combined with 25.00 mL of toluene (0.05 mol L⁻¹ *n*-butylamine solution) into conical flask (250 mL). After shaking for 5 min under cover, 2-proponal (100 mL) and bromophenol blue sodium salt (1 drop of diluted solution) are added too. Then, this mixture is titrated by HCl solution (0.025 mol L⁻¹), and the end point arrives when solution color is changed from blue to yellow. The acid amount of solid sample is the adsorbed amount of *n*-butylamine, which is obtained by subtraction of total *n*-butylamine with the residues in solution that determined by HCl titration.

12. FT-IR spectra of synthetic samples

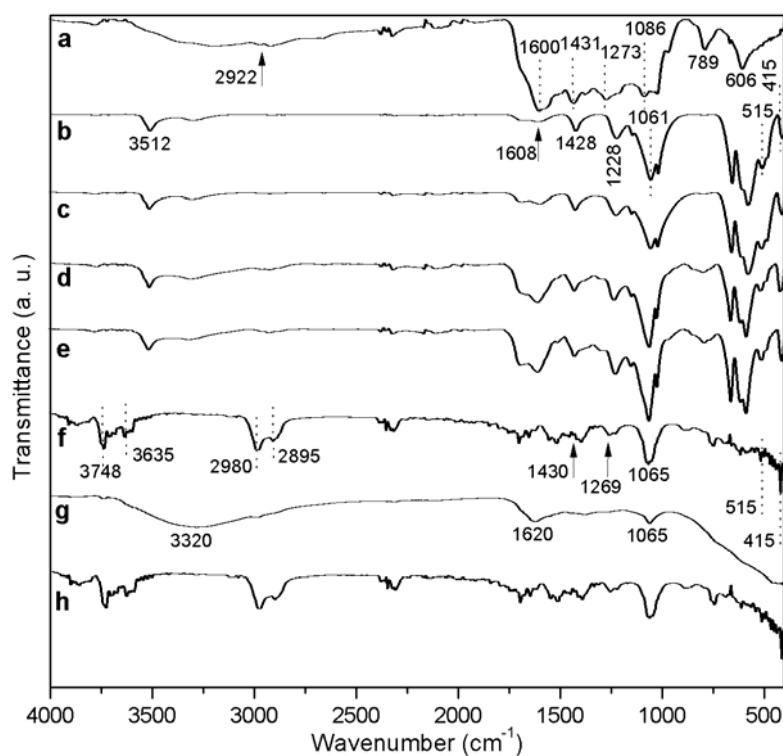
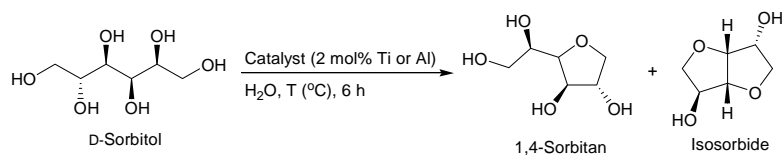


Fig. S11 FT-IR spectra of synthetic samples.

(a) C1; (b) C2; (c) C3; (d) C4; (e) C5; (f) C6; (g) C7; (h) C8.

13. Catalytic dehydration of D-sorbitol to fine chemicals in water

Table S1 Catalytic dehydration of D-sorbitol to fine chemicals in water



Entry ^{a)}	Catalyst	Temperature/ ^o C	Conversion ^{b)} /%	Yield of 1,4-sorbitan ^{c)} /%	Yield of isosorbide ^{d)} /%
1	Al ₂ O ₃	20	7	5	2
2		80	11	9	2
3	C2	20	8	5	3
4		80	10	8	2
5	C3	20	6	5	1
6		80	9	7	2
7	C4	20	9	8	1
8		80	14	11	3
9	C5	20	10	8	2
10		80	15	11	4
11	C6	20	13	13	0
12		80	5	5	0
13	C7	20	4	4	0
14		80	8	8	0
15	C8	20	4	4	0
16		80	12	12	0

Notes: a) Conditions as in Sect. 2.4; b) conversion of D-sorbitol to all dehydrated products, determined by GC-MS (Sect. 17, Supplementary material); c) yield of 1,4-sorbitan based on substrate, determined by GC-MS (Sect. 17, Supplementary material); d) yield of isosorbide based on substrate, determined by GC-MS (Sect. 17, Supplementary material)

14. Catalyst recycling and real-time UV monitoring

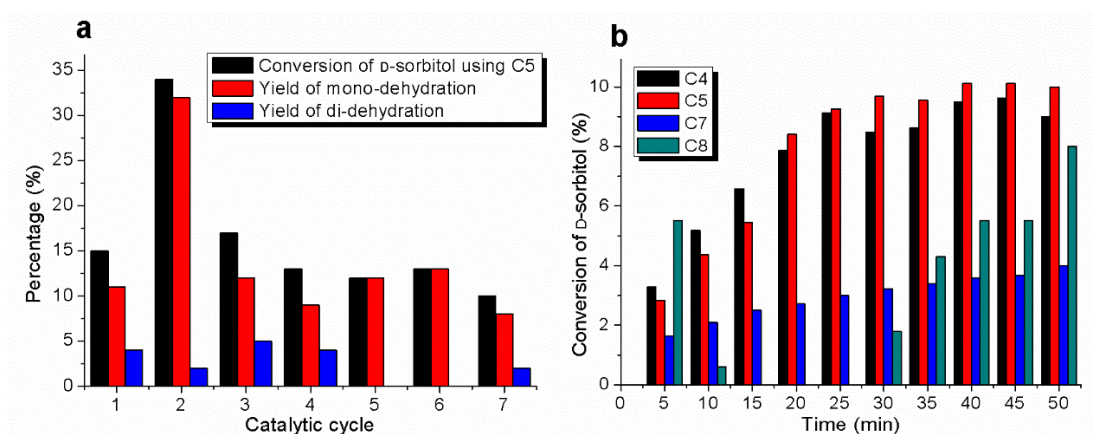


Fig. S12 Catalyst recycling and real-time UV monitoring.

(a) Recycling of C5 according to profile of entry 10, Table S; (b) real-time UV monitoring dehydration of D-sorbitol using C4, C5, C7 and C8 according to profiles of entries 7, 9, 13, and 15, Table S1.

15. UV-Vis monitoring catalytic solution

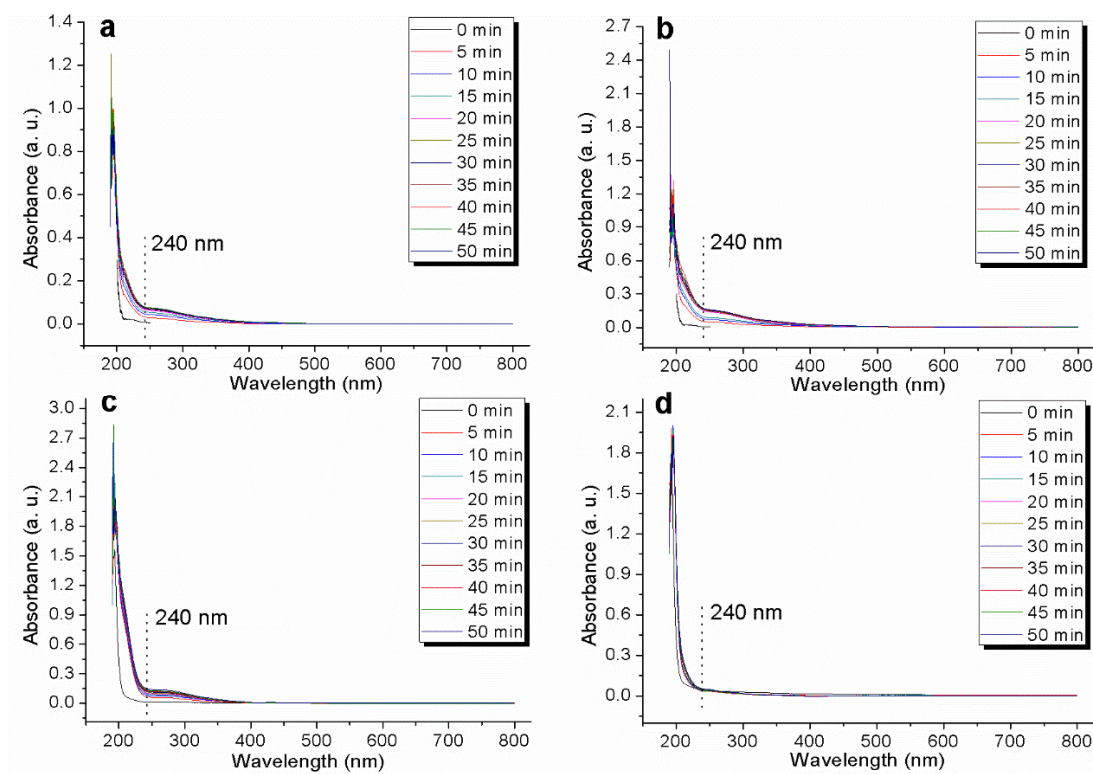


Fig. S13 UV-Vis monitoring catalytic solution according to profiles of entries 7, 9, 13, and 15, Table S1

(a) Using C4, (b) using C5, (c) using C7, (d) using C8

16. The calculated contour of HOMO and LUMO for transition states TS8-TS11

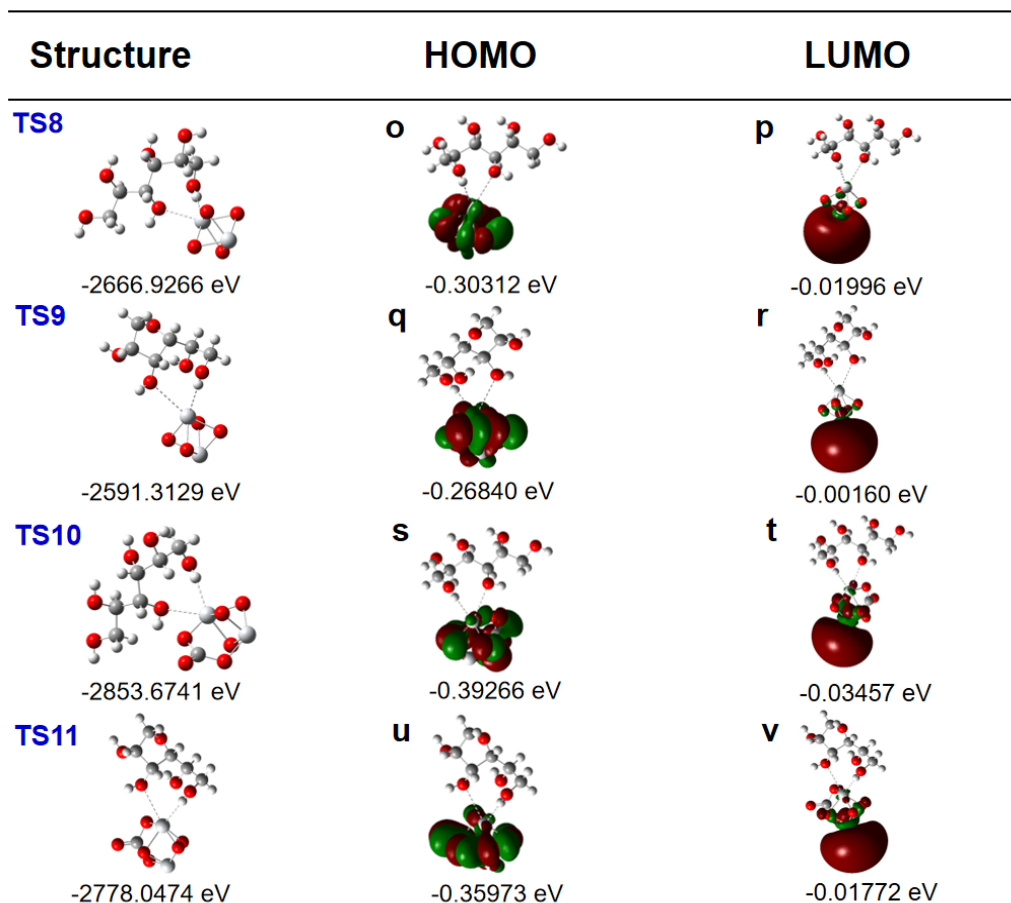


Fig. S14 The calculated contour of HOMO and LUMO for transition states TS8-TS11 in proposed mechanism.

17. GC-MS examples for Table S1

(1) Entry 1, Table S1

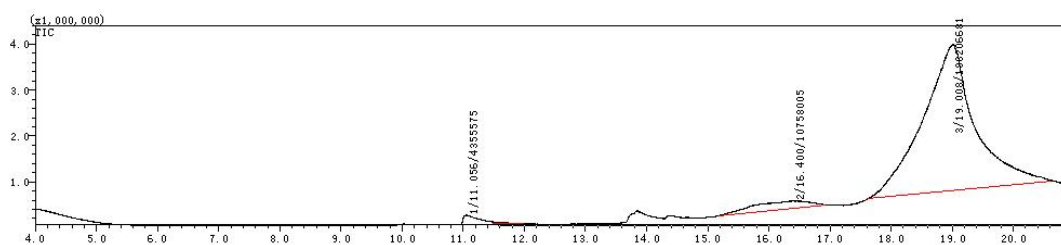
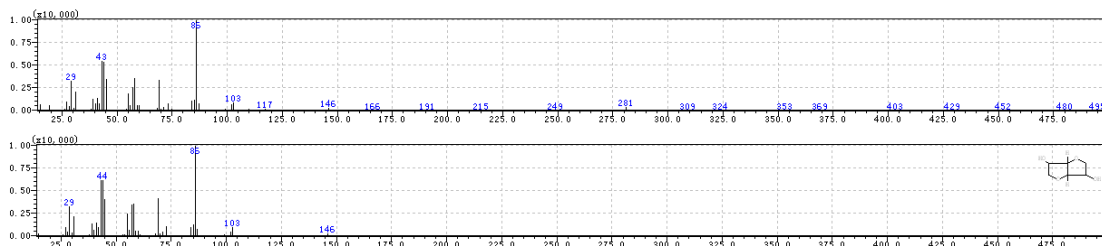


Fig. S15 GC part of GC-MS for Entry 1, Table S1.

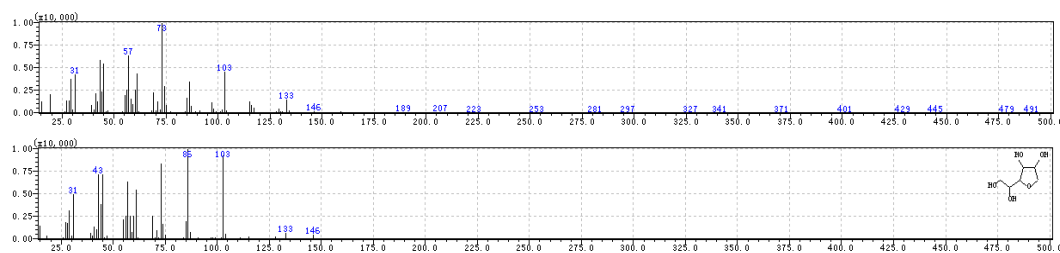
In this image, data format is peak number/retention time(min)/integral area.

The peak for $t_R = 11.056$ min is:



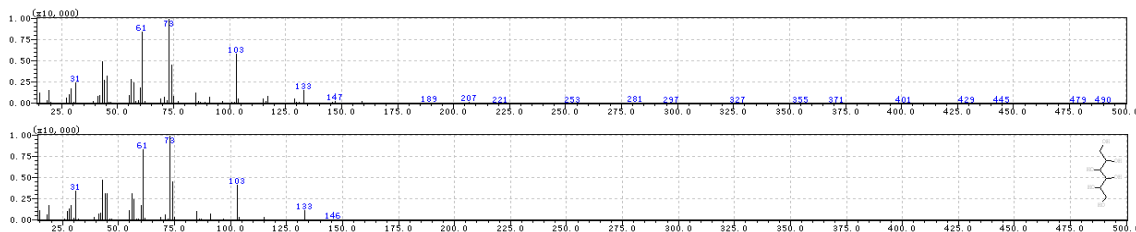
GC-MS: calcd. for $C_6H_{10}O_4$ 146, found 146 ($C_6H_{10}O_4$). Isosorbide.

The peak for $t_R = 16.400$ min:



GC-MS: calcd. for $C_6H_{12}O_5$ 164, found 146 ($C_6H_{12}O_5 - H_2O$). 1,4-Sorbitan.

The peak for $t_R = 19.008$ min:



GC-MS: calcd. for $C_6H_{14}O_6$ 182, found 147 ($C_6H_{14}O_6 - H_2O - OH$). The unreacted D-sorbitol.

(2) Entry 2, Table S1

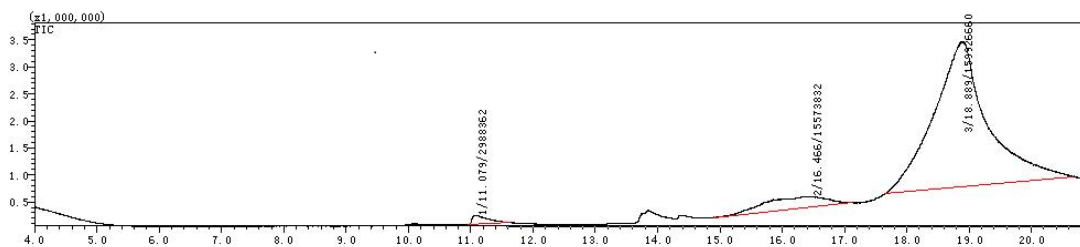


Fig. S16 GC part of GC-MS for Entry 2, Table S1.

The peak at $t_R = 11.079$ min is isosorbide. That at 16.466 min is 1,4-sorbitan, while that at 18.889 min is unreacted D-sorbitol.

(3) Entry 3, Table S1

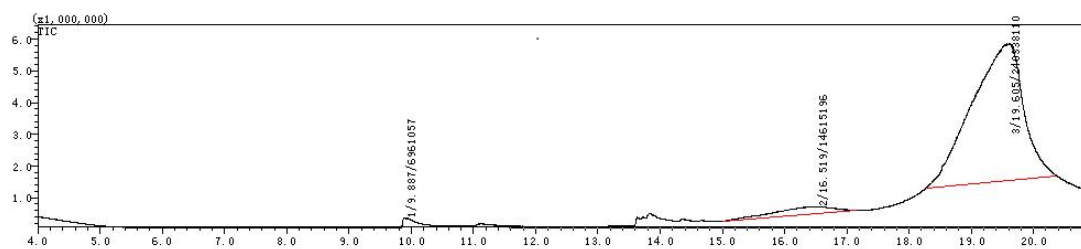


Fig. S17 GC part of GC-MS for Entry 3, Table S1.

The peak at $t_R = 9.887$ min is isosorbide. That at 16.519 min is 1,4-sorbitan, while that at 19.605 min is unreacted D-sorbitol.

(4) Entry 4, Table S1

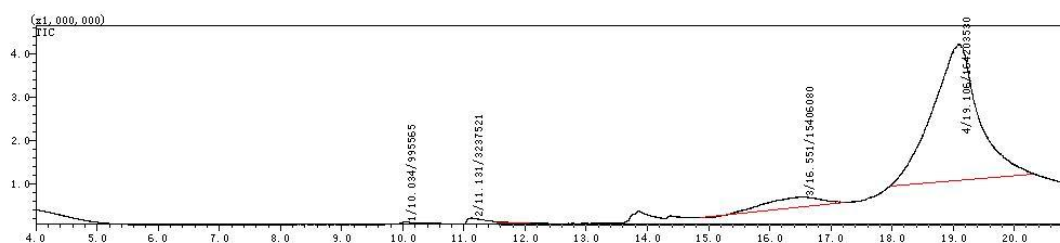


Fig. S18 GC part of GC-MS for Entry 4, Table S1.

The peaks at $t_R = 10.034$ min and 11.131 min are both isosorbide. That at 16.551 min is 1,4-sorbitan, while that at 19.106 min is unreacted D-sorbitol.

(5) Entry 5, Table S1

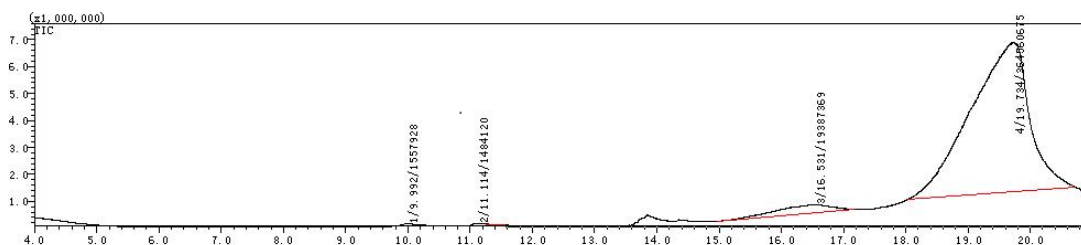


Fig. S19 GC part of GC-MS for Entry 5, Table S1.

The peaks at $t_R = 9.992$ min and 11.114 min are both isosorbide. That at 16.531 min is 1,4-sorbitan, while that at 19.734 min is unreacted D-sorbitol.

(6) Entry 6, Table S1

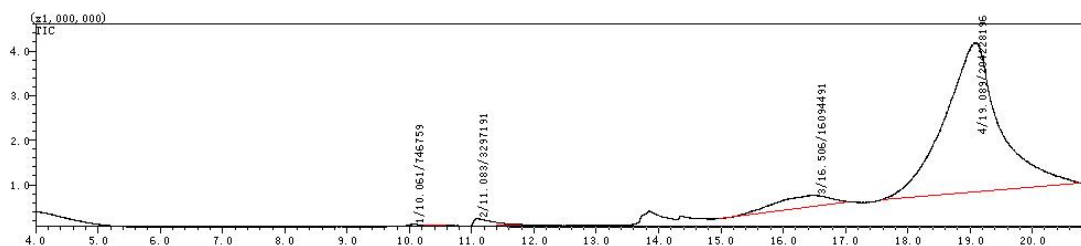


Fig. S20 GC part of GC-MS for Entry 6, Table S1.

The peaks at $t_R = 10.061$ min and 11.083 min are both isosorbide. That at 16.506 min is 1,4-sorbitan, while that at 19.089 min is unreacted D-sorbitol.

(7) Entry 7, Table S1

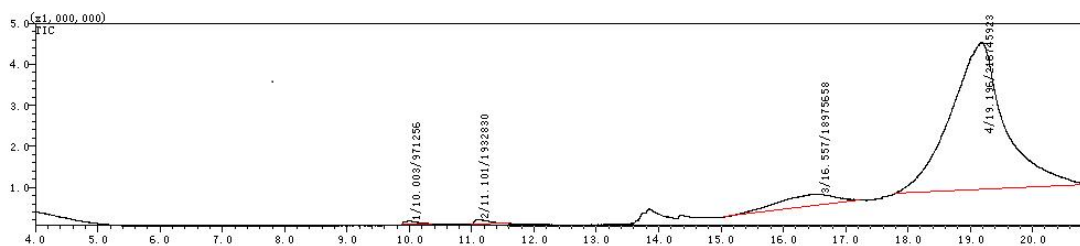


Fig. S21 GC part of GC-MS for Entry 7, Table S1.

The peaks at $t_R = 10.003$ min and 11.101 min are both isosorbide. That at 16.557 min is 1,4-sorbitan, while that at 19.196 min is unreacted D-sorbitol.

(8) Entry 8, Table S1

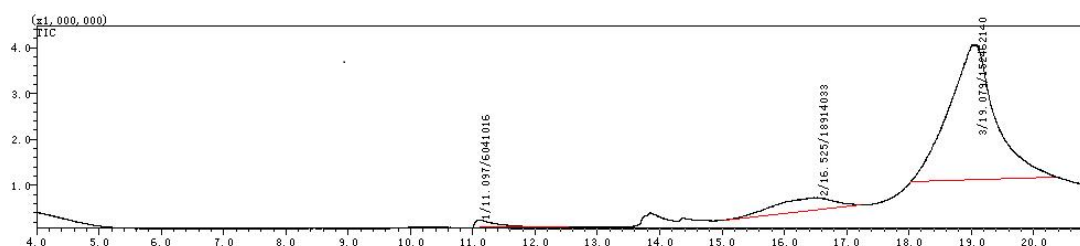


Fig. S22 GC part of GC-MS for Entry 8, Table S1.

The peak at $t_R = 11.097$ min is isosorbide. That at 16.525 min is 1,4-sorbitan, while that at 19.079 min is unreacted D-sorbitol.

(9) Entry 9, Table S1

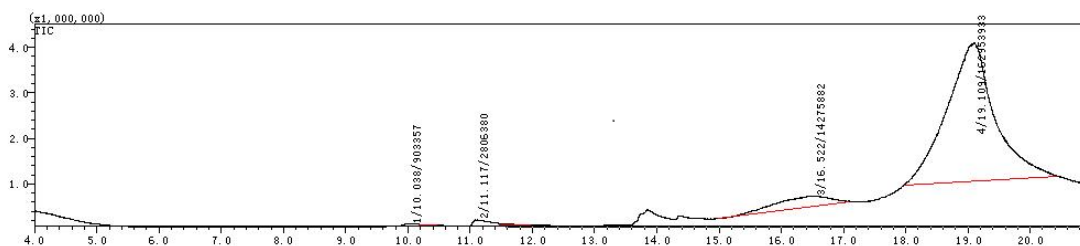


Fig. S23 GC part of GC-MS for Entry 9, Table S1.

The peaks at $t_R = 10.038$ min and 11.117 min are both isosorbide. That at 16.522 min is 1,4-sorbitan, while that at 19.109 min is unreacted D-sorbitol.

(10) Entry 10, Table S1

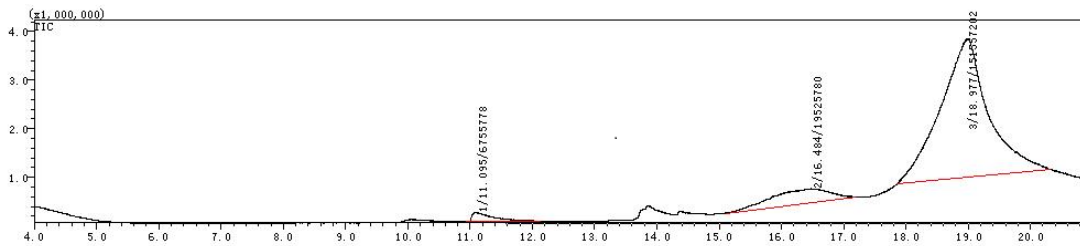


Fig. S24 GC part of GC-MS for Entry 10, Table S1.

The peak at $t_R = 11.095$ min is isosorbide. That at 16.484 min is 1,4-sorbitan, while that at 18.977 min is unreacted D-sorbitol.

(11) Entry 11, Table S1

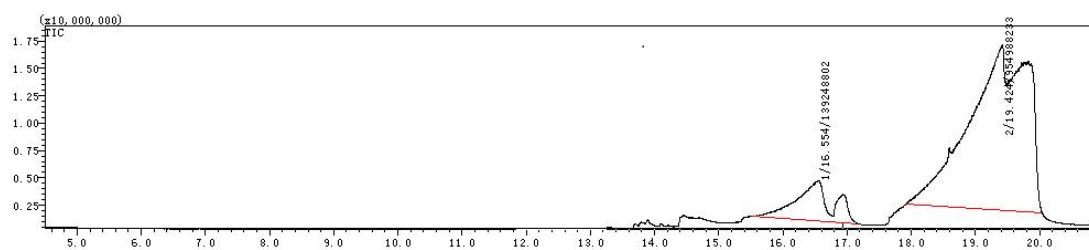


Fig. S25 GC part of GC-MS for Entry 11, Table S1.

The peak at $t_R = 16.554$ min is 1,4-sorbitan, while that at 19.424 min is unreacted D-sorbitol.

(12) Entry 12, Table S1

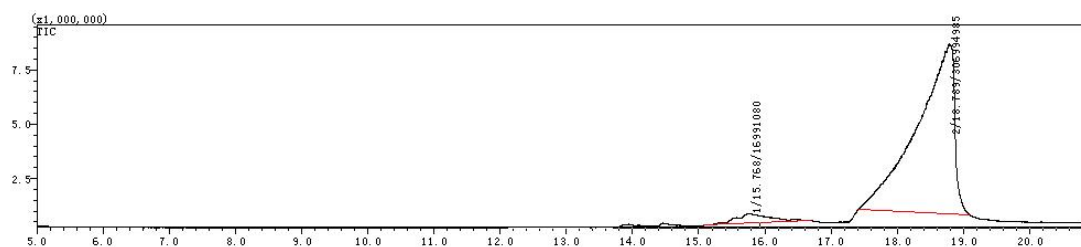


Fig. S26 GC part of GC-MS for Entry 12, Table S1.

The peak at $t_R = 15.768$ min is 1,4-sorbitan, while that at 18.769 min is unreacted D-sorbitol.

(13) Entry 13, Table S1

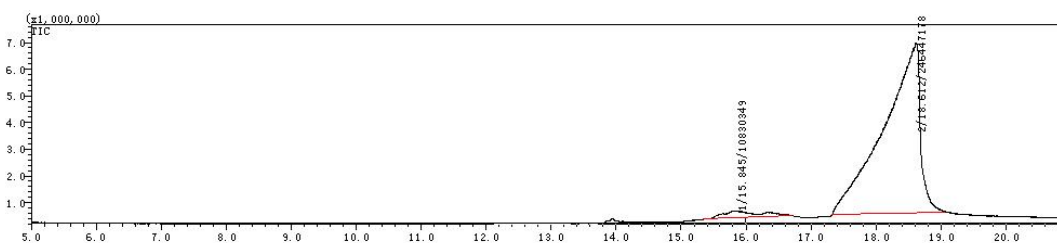


Fig. S27 GC part of GC-MS for Entry 13, Table S1.

The peak at $t_R = 15.768$ min is 1,4-sorbitan, while that at 18.769 min is unreacted D-sorbitol.

(14) Entry 14, Table S1

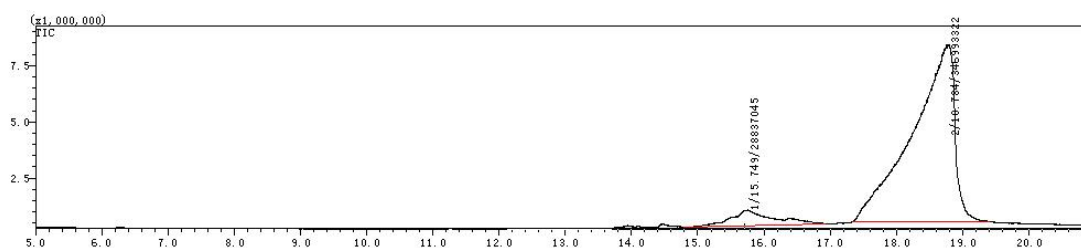


Fig. S28 GC part of GC-MS for Entry 14, Table S1.

The peak at $t_R = 15.749$ min is 1,4-sorbitan, while that at 18.784 min is unreacted D-sorbitol.

(15) Entry 15, Table S1

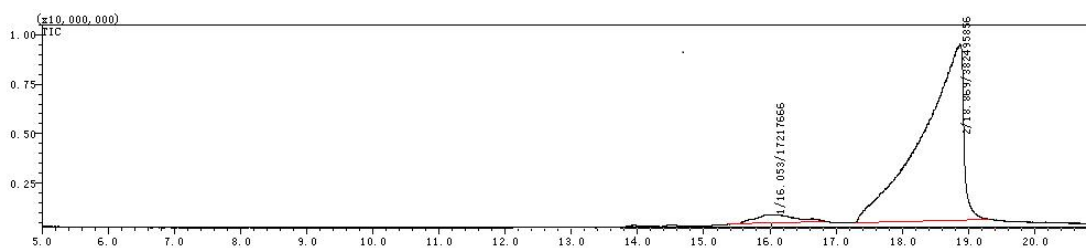


Fig. S29 GC part of GC-MS for Entry 15, Table S1.

The peak at $t_R = 16.053$ min is 1,4-sorbitan, while that at 18.869 min is unreacted D-sorbitol.

(16) Entry 16, Table S1

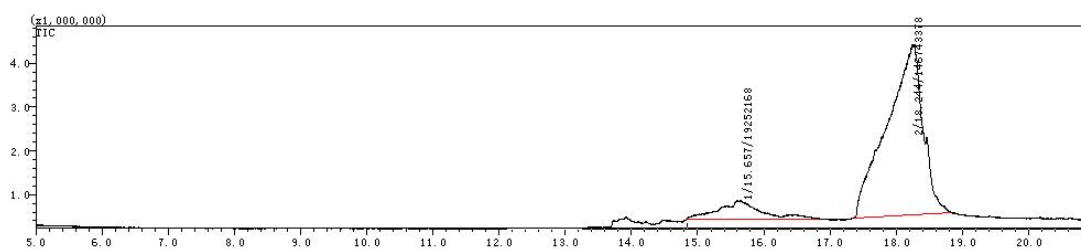


Fig. S30 GC part of GC-MS for Entry 16, Table S1.

The peak at $t_R = 15.657$ min is 1,4-sorbitan, while that at 18.344 min is unreacted D-sorbitol.

18. GC-MS examples for Table 3

(17) Entry 1, Table 3

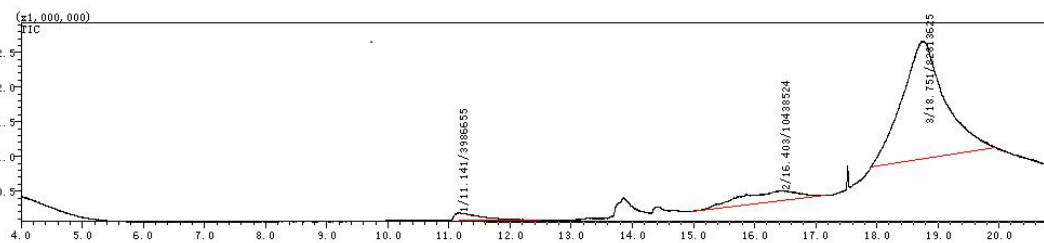


Fig. S31 GC part of GC-MS for Entry 1, Table 3.

The peak at $t_R = 11.141$ min is isosorbide. That at 16.403 min is 1,4-sorbitan, while that at 18.751 min is unreacted D-sorbitol.

(18) Entry 2, Table 3

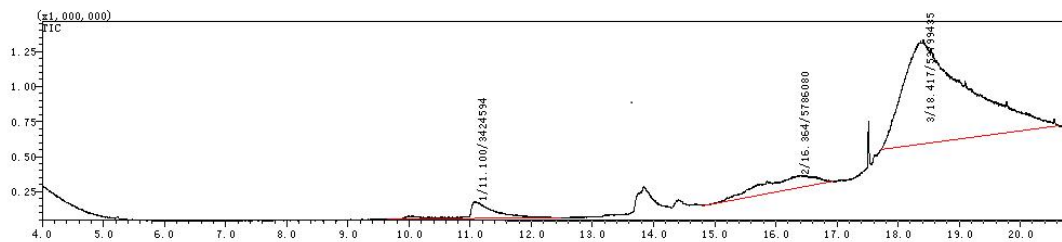


Fig. S32 GC part of GC-MS for Entry 2, Table 3.

The peak at $t_R = 11.100$ min is isosorbide. That at 16.364 min is 1,4-sorbitan, while that at 18.417 min is unreacted D-sorbitol.

(19) Entry 3, Table 3

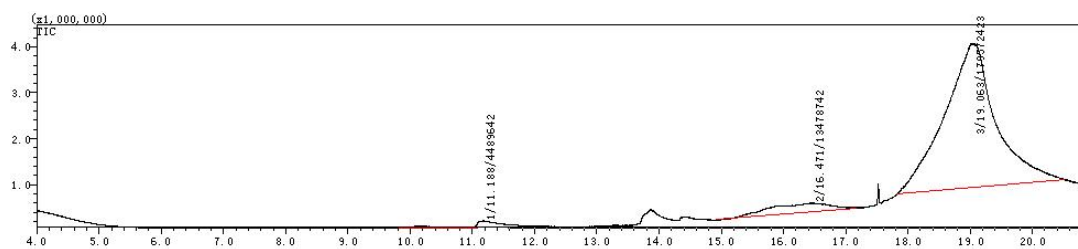


Fig. S33 GC part of GC-MS for Entry 3, Table 3.

The peak at $t_R = 11.188$ min is isosorbide. That at 16.471 min is 1,4-sorbitan, while that at 19.063 min is unreacted D-sorbitol.

(20) Entry 4, Table 3

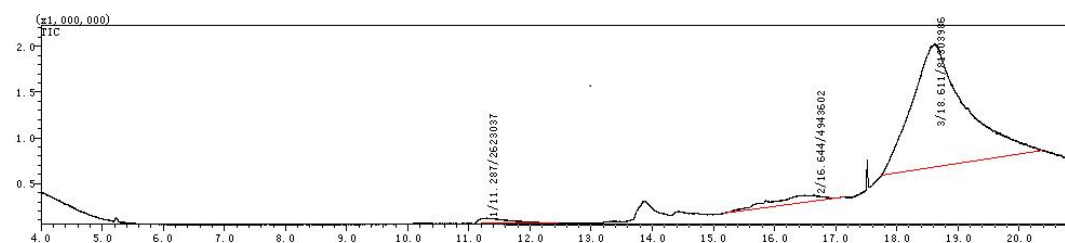


Fig. S34 GC part of GC-MS for Entry 4, Table 3.

The peak at $t_R = 11.287$ min is isosorbide. That at 16.644 min is 1,4-sorbitan, while that at 18.611 min is unreacted D-sorbitol.

(21) Entry 5, Table 3

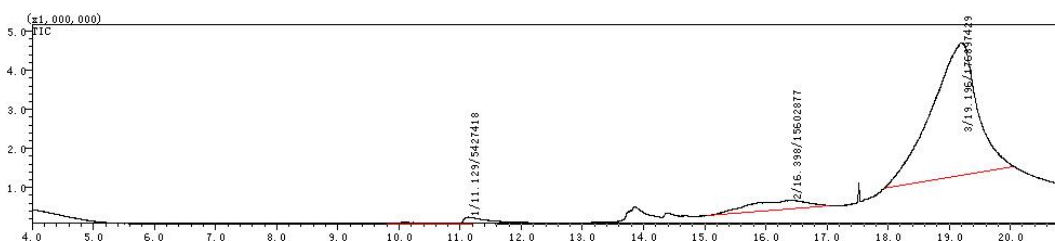


Fig. S35 GC part of GC-MS for Entry 5, Table 3.

The peak at $t_R = 11.129$ min is isosorbide. That at 16.398 min is 1,4-sorbitan, while that at 19.196 min is unreacted D-sorbitol.

(22) Entry 6, Table 3

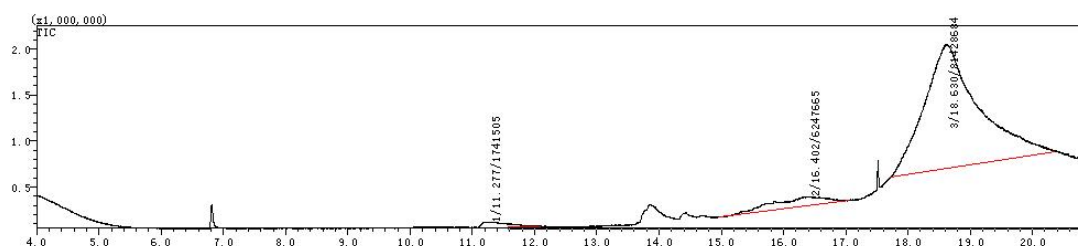


Fig. S36 GC part of GC-MS for Entry 6, Table 3.

The peak at $t_R = 11.129$ min is isosorbide. That at 16.402 min is 1,4-sorbitan, while that at 18.630 min is unreacted D-sorbitol.

(23) Entry 7, Table 3

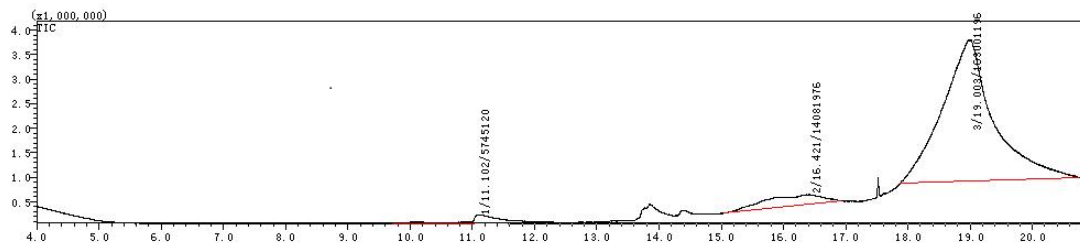


Fig. S37 GC part of GC-MS for Entry 7, Table 3.

The peak at $t_R = 11.102$ min is isosorbide. That at 16.421 min is 1,4-sorbitan, while that at 19.003 min is unreacted D-sorbitol.

(24) Entry 8, Table 3

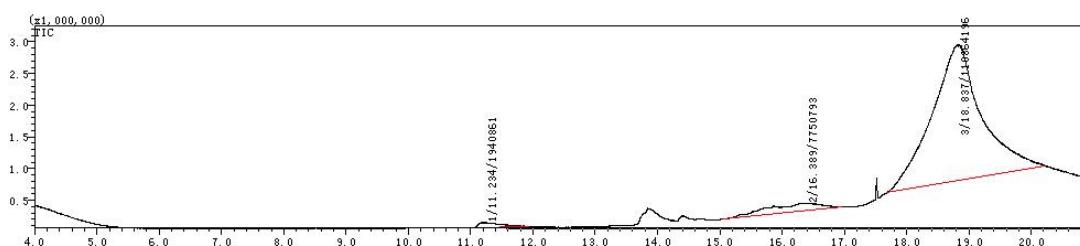


Fig. S38 GC part of GC-MS for Entry 8, Table 3.

The peak at $t_R = 11.234$ min is isosorbide. That at 16.389 min is 1,4-sorbitan, while that at 18.837 min is unreacted D-sorbitol.

(25) Entry 9, Table 3

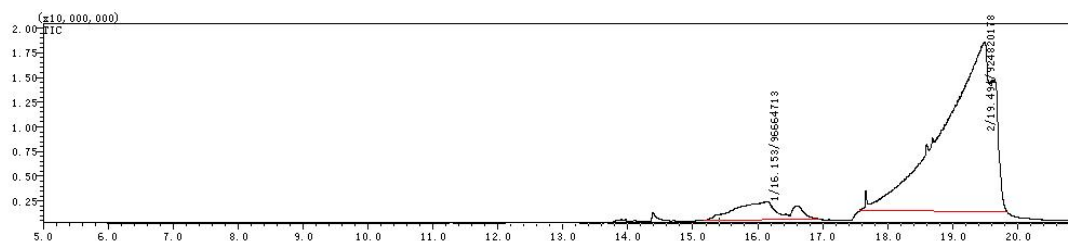


Fig. S39 GC part of GC-MS for Entry 9, Table 3.

The peak at $t_R = 16.153$ min is 1,4-sorbitan, while that at 19.494 min is unreacted D-sorbitol.

(26) Entry 10, Table 3

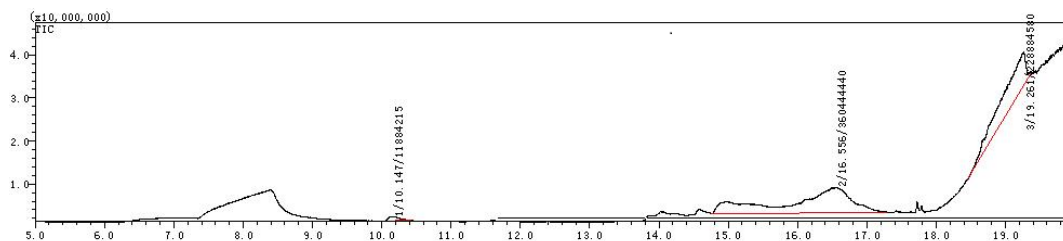


Fig. S40 GC part of GC-MS for Entry 10, Table 3.

The peak at $t_R = 10.147$ min is isosorbide. That at 16.556 min is 1,4-sorbitan, while that at 19.261 min is unreacted D-sorbitol.

(27) Entry 11, Table 3

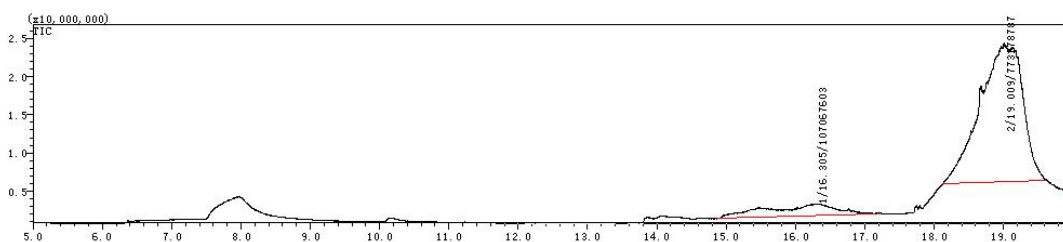


Fig. S41 GC part of GC-MS for Entry 11, Table 3.

The peak at 16.305 min is 1,4-sorbitan, while that at 19.009 min is unreacted D-sorbitol.

(28) Entry 12, Table 3

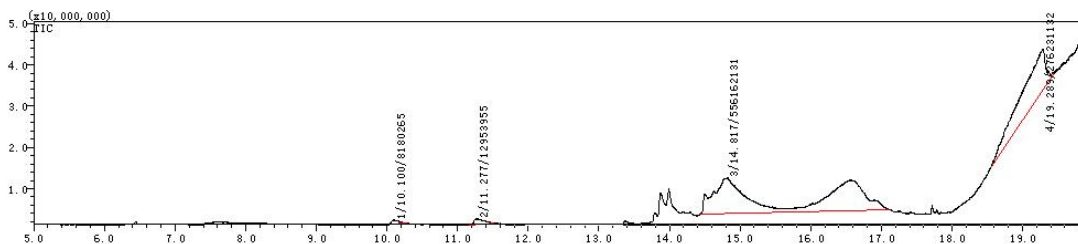


Fig. S42 GC part of GC-MS for Entry 12, Table 3.

The peaks at $t_R = 10.100$ and 11.277 min are both isosorbide. That at 14.817 min is 1,4-sorbitan, while that at 19.289 min is unreacted D-sorbitol.

(29) Entry 13, Table 3

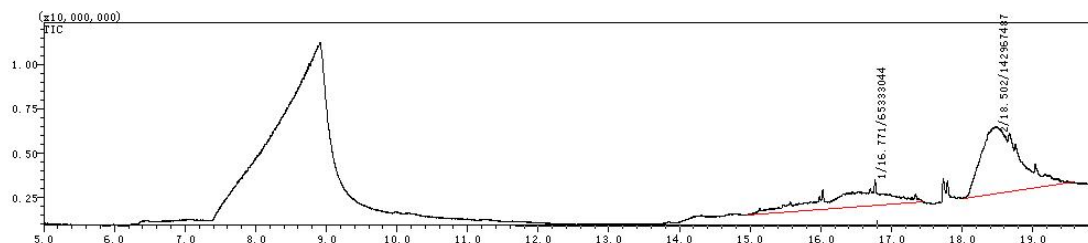


Fig. S43 GC part of GC-MS for Entry 13, Table 3.

The peak at $t_R = 16.771$ min is 1,4-sorbitan, while that at 18.502 min is unreacted D-sorbitol.

(30) Entry 14, Table 3

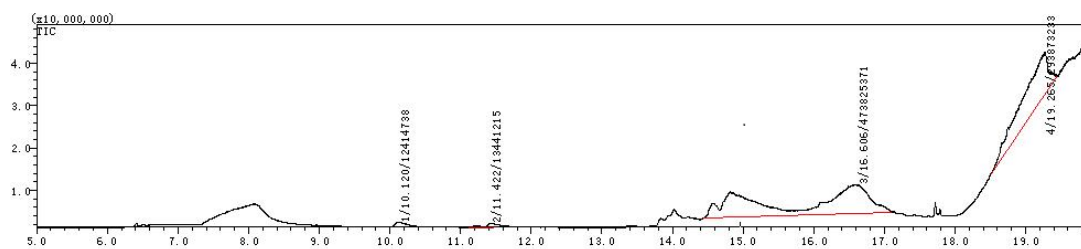


Fig. S44 GC part of GC-MS for Entry 14, Table 3.

The peaks at $t_R = 10.120$ and 11.422 min are both isosorbide. That at 16.606 min is 1,4-sorbitan, while that at 19.265 min is unreacted D-sorbitol.

19. GC-MS examples for Table 4

(31) Entry 15, Table 4

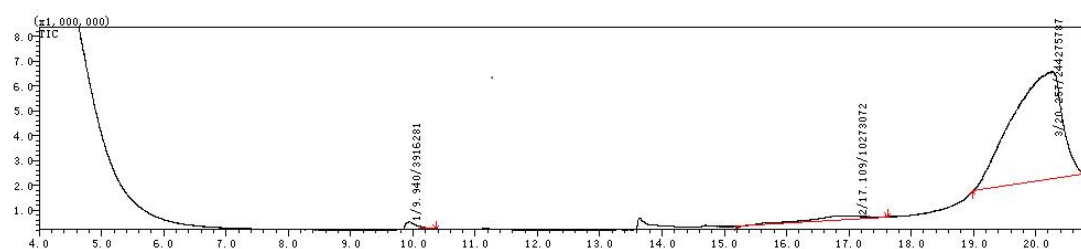
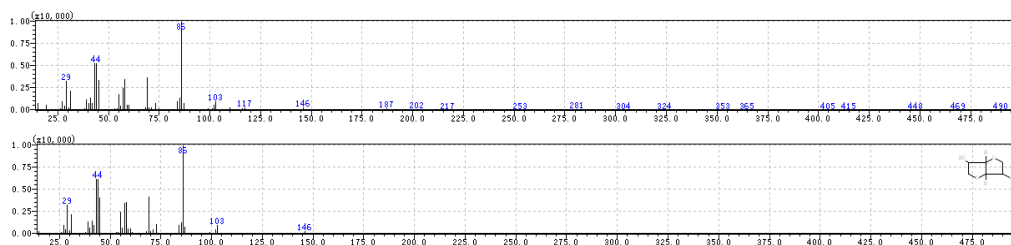


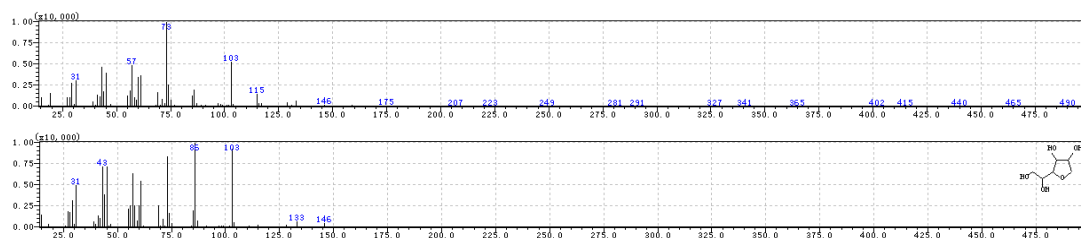
Fig. S45 GC part of GC-MS for Entry 15, Table 4.

The peak at $t_R = 9.940$ min is isomannide:



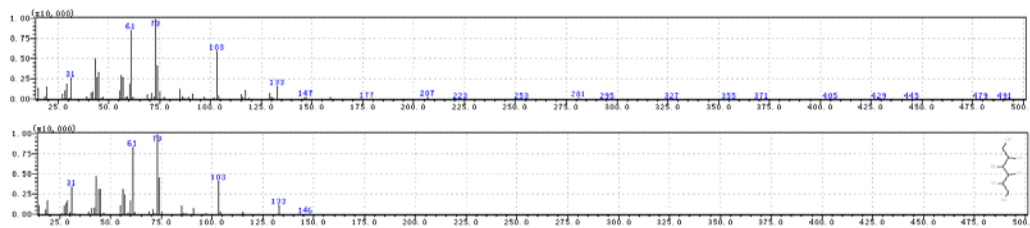
GC-MS: calcd. for $C_6H_{10}O_4$ 146, found 146 ($C_6H_{10}O_4$).

The peak at $t_R = 17.109$ min is 1,4-mannitan:



GC-MS: calcd. for $C_6H_{12}O_5$ 164, found 146 ($C_6H_{12}O_5 - H_2O$).

That at $t_R = 20.257$ min is the unreacted D-mannitol:



GC-MS: calcd. for $C_6H_{14}O_6$ 182, found 147 ($C_6H_{14}O_6 - H_2O - OH$).

(32) Entry 16, Table 4

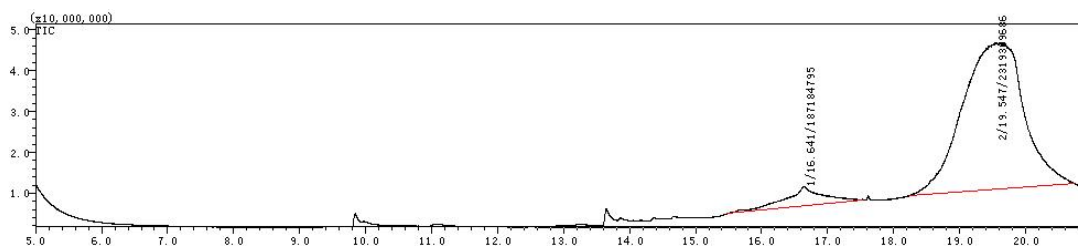


Fig. S46 GC part of GC-MS for Entry 16, Table 4.

The peak at $t_R = 16.641$ min is 1,4-mannitan, while that at $t_R = 19.547$ min is the unreacted D-mannitol.

(33) Entry 17, Table 4

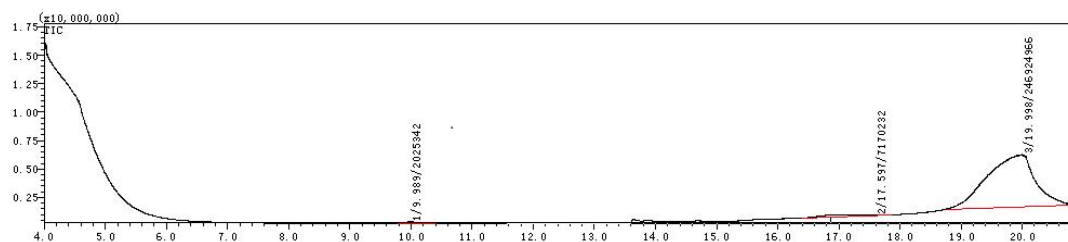


Fig. S47 GC part of GC-MS for Entry 17, Table 4.

The peak at $t_R = 9.989$ min is isomannide, that at $t_R = 17.597$ min is 1,4-mannitan, while that at $t_R = 19.998$ min is the unreacted D-mannitol.

(34) Entry 18, Table 4

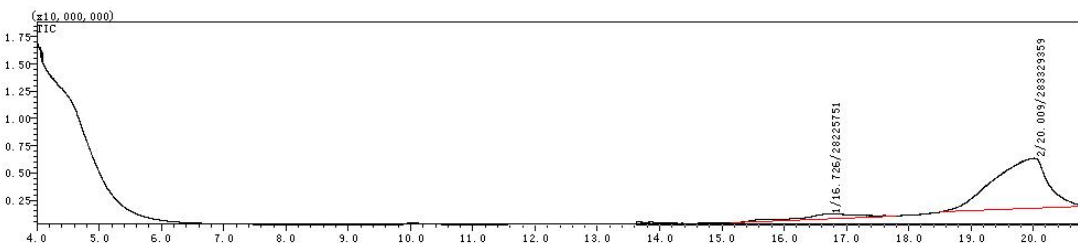


Fig. S48 GC part of GC-MS for Entry 18, Table 4.

The peak at $t_R = 16.726$ min is 1,4-mannitan, while that at $t_R = 20.009$ min is the unreacted D-mannitol.

(35) Entry 19, Table 4

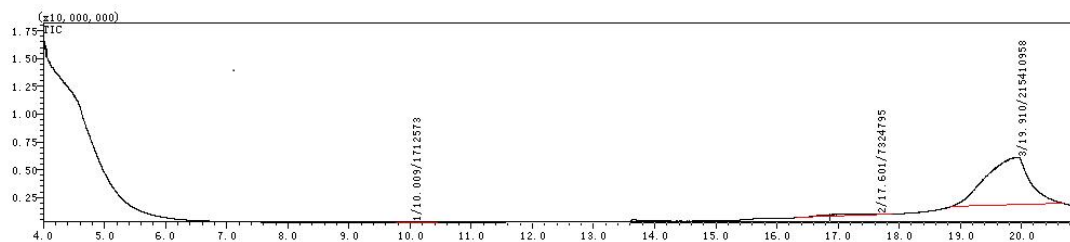


Fig. S49 GC part of GC-MS for Entry 19, Table 4.

The peak at $t_R = 10.009$ min is isomannide, that at $t_R = 17.601$ min is 1,4-mannitan, while that at $t_R = 19.910$ min is the unreacted D-mannitol.

(36) Entry 20, Table 4

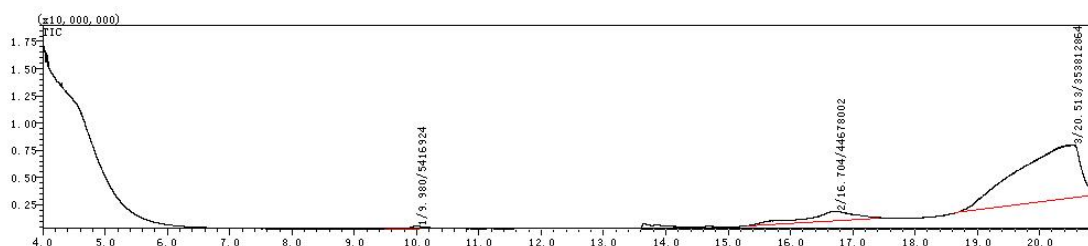


Fig. S50 GC part of GC-MS for Entry 20, Table 4.

The peak at $t_R = 9.980$ min is isomannide, that at $t_R = 16.704$ min is 1,4-mannitan, while that at $t_R = 20.513$ min is the unreacted D-mannitol.

(37) Entry 21, Table 4

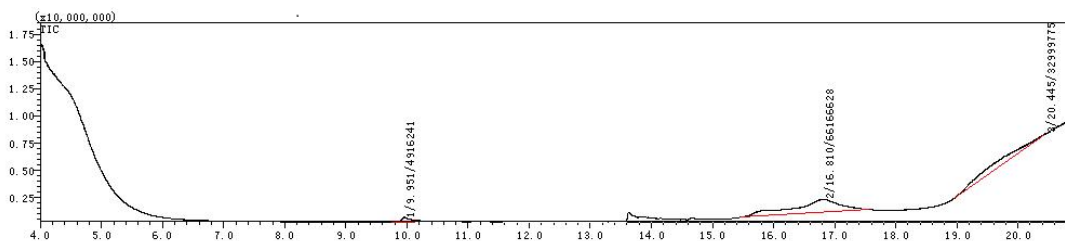


Fig. S51 GC part of GC-MS for Entry 21, Table 4.

The peak at $t_R = 9.951$ min is isomannide, that at $t_R = 16.810$ min is 1,4-mannitan, while that at $t_R = 20.445$ min is the unreacted D-mannitol.

(38) Entry 22, Table 4

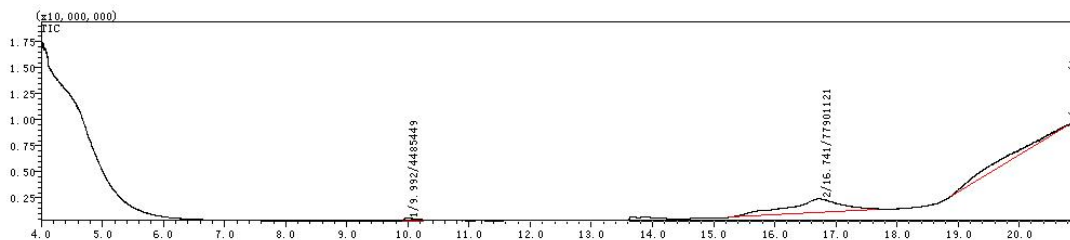


Fig. S52 GC part of GC-MS for Entry 22, Table 4.

The peak at $t_R = 9.992$ min is isomannide, that at $t_R = 16.741$ min is 1,4-mannitan, while that at $t_R = 20.733$ min is the unreacted D-mannitol.

(39) Entry 23, Table 4

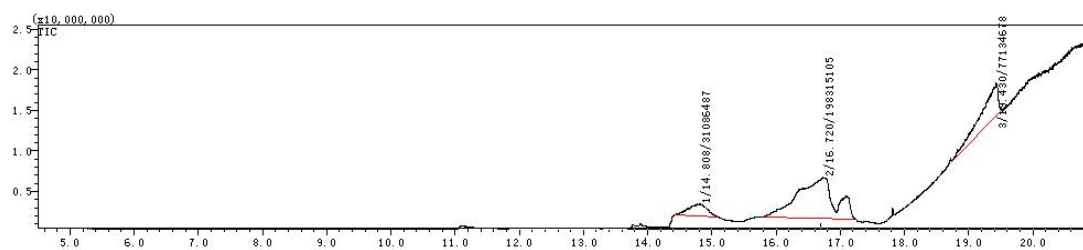


Fig. S53 GC part of GC-MS for Entry 23, Table 4.

The peaks at $t_R = 14.808$ and 16.720 min are both 1,4-mannitan, while that at $t_R = 19.430$ min is the unreacted D-mannitol.

(40) Entry 24, Table 4

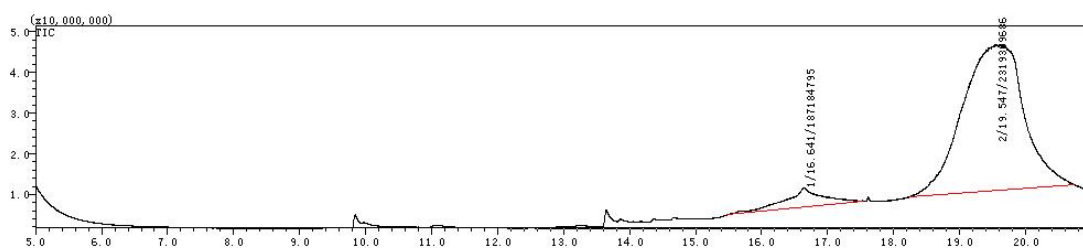


Fig. S54 GC part of GC-MS for Entry 24, Table 4.

The peak at $t_R = 16.641$ min is 1,4-mannitan, while that at $t_R = 19.547$ min is the unreacted D-mannitol.

(41) Entry 25, Table 4

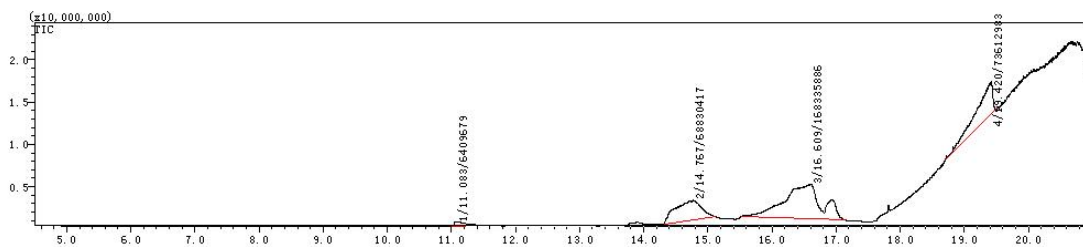


Fig. S55 GC part of GC-MS for Entry 25, Table 4.

The peak at $t_R = 11.083$ min is isomannide, that at $t_R = 14.767$ and 16.609 min are both 1,4-mannitan, while that at $t_R = 19.420$ min is the unreacted D-mannitol.

(42) Entry 26, Table 4

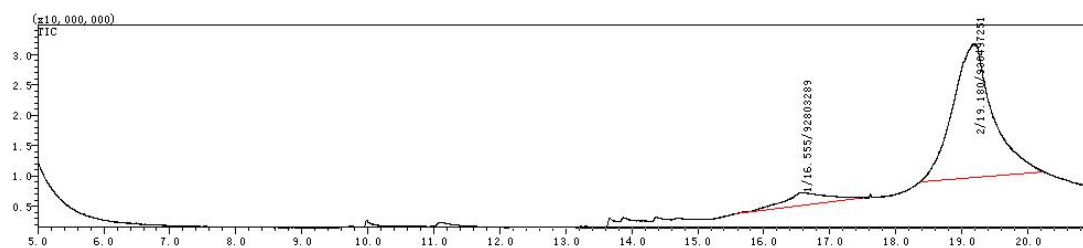


Fig. S56 GC part of GC-MS for Entry 26, Table 4.

The peak at $t_R = 16.555$ min is 1,4-mannitan, while that at $t_R = 19.180$ min is the unreacted D-mannitol.

(43) Entry 27, Table 4

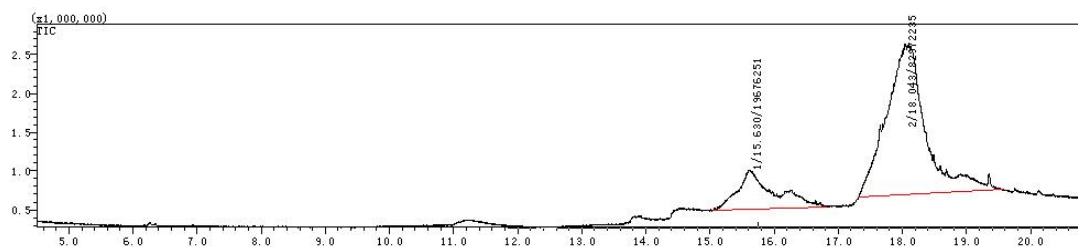


Fig. S57 GC part of GC-MS for Entry 27, Table 4.

The peak at $t_R = 16.555$ min is 1,4-mannitan, while that at $t_R = 19.180$ min is the unreacted D-mannitol.

(44) Entry 28, Table 4

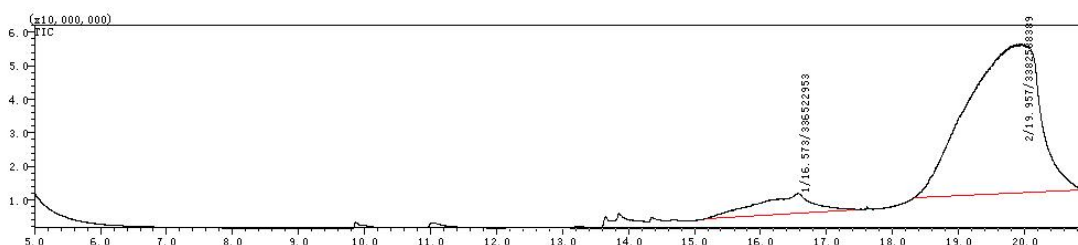


Fig. S58 GC part of GC-MS for Entry 28, Table 4.

The peak at $t_R = 16.573$ min is 1,4-mannitan, while that at $t_R = 19.957$ min is the unreacted D-mannitol.

20. GC-MS examples for Table 5

(45) Entry 29, Table 5

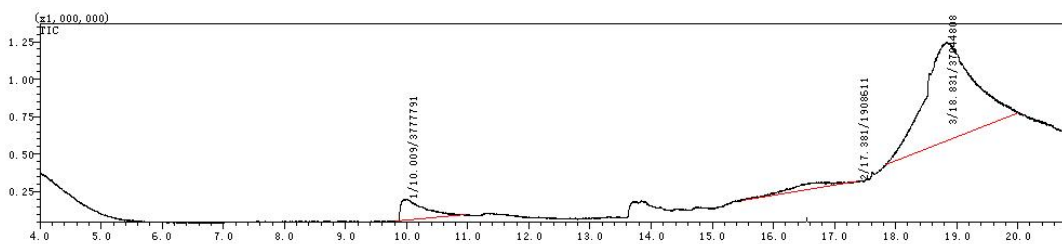


Fig. S59 GC part of GC-MS for Entry 29, Table 5.

The peak at $t_R = 10.009$ min is isomannide, that at $t_R = 17.381$ min is 1,4-mannitan, while that at $t_R = 18.831$ min is the unreacted D-mannitol.

(46) Entry 30, Table 5

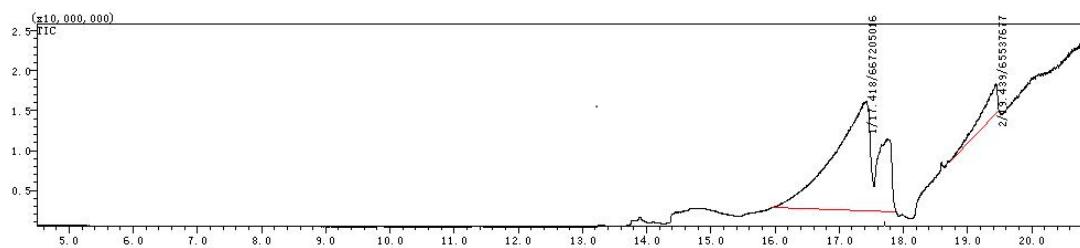


Fig. S60 GC part of GC-MS for Entry 30, Table 5.

The peak at $t_R = 17.418$ min is 1,4-mannitan, while that at $t_R = 19.439$ min is the unreacted D-mannitol.

(47) Entry 31, Table 5

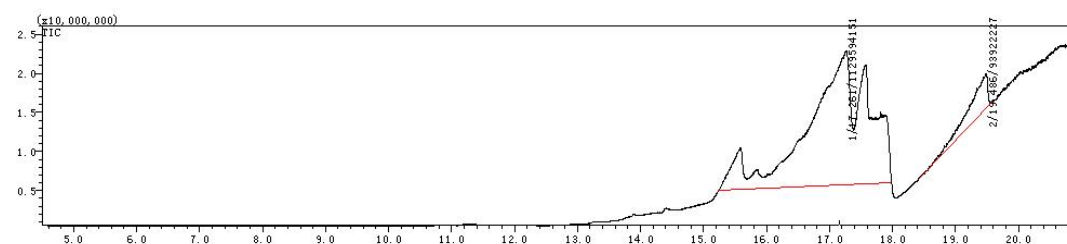


Fig. S61 GC part of GC-MS for Entry 31, Table 5.

The peak at $t_R = 17.261$ min is 1,4-mannitan, while that at $t_R = 19.486$ min is the unreacted D-mannitol.

(48) Entry 32, Table 5

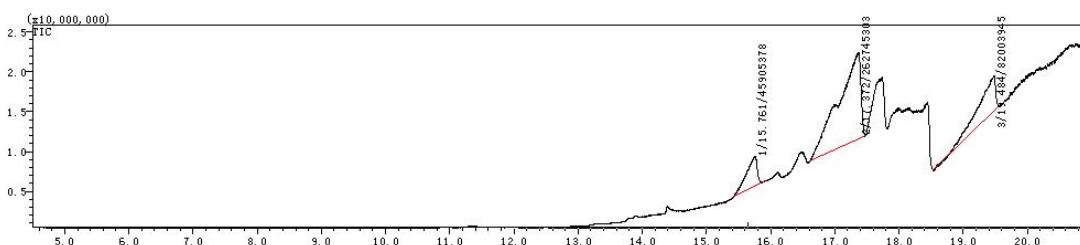


Fig. S62 GC part of GC-MS for Entry 32, Table 5.

The peaks at $t_R = 15.761$ and 17.372 min are both 1,4-mannitan, while that at $t_R = 19.484$ min is the unreacted D-mannitol.

(49) Entry 33, Table 5

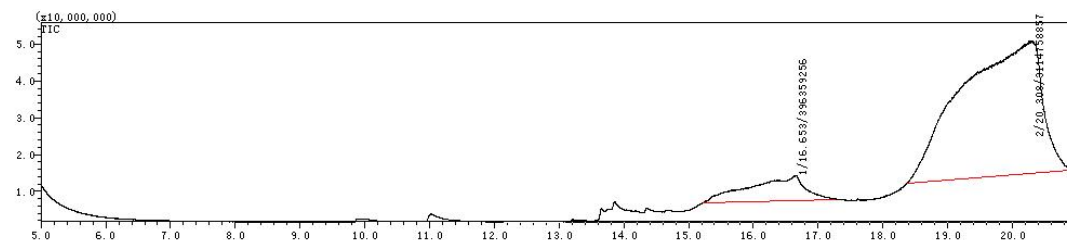


Fig. S63 GC part of GC-MS for Entry 33, Table 5.

The peak at $t_R = 16.653$ min is 1,4-mannitan, while that at $t_R = 20.303$ min is the unreacted D-mannitol.

(50) Entry 34, Table 5

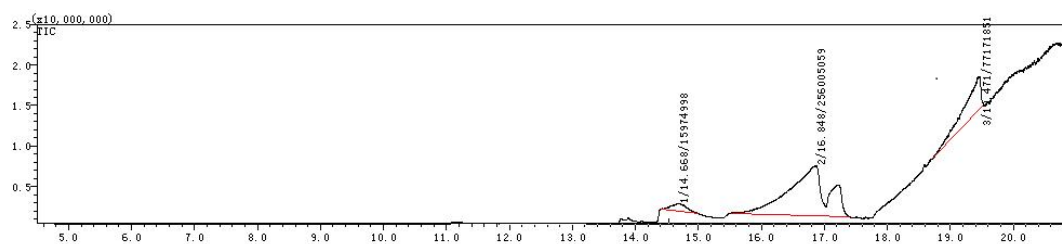


Fig. S64 GC part of GC-MS for Entry 34, Table 5.

The peaks at $t_R = 14.668$ and 16.848 min are both 1,4-mannitan, while that at $t_R = 19.471$ min is the unreacted D-mannitol.

21. GC-MS examples for recycling

(a) Cycle 2, a, Fig. S12

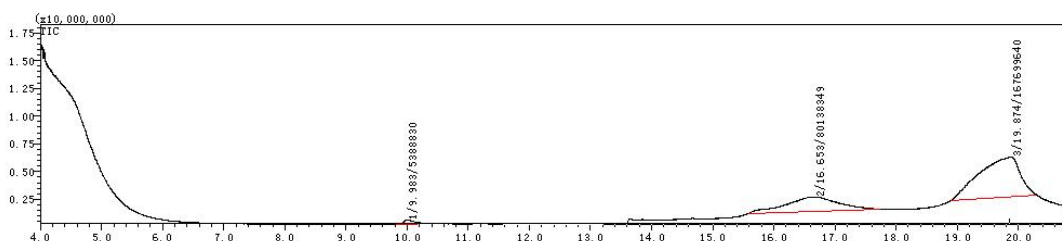


Fig. S65 GC part of GC-MS for Cycle 2, a, Fig. S12.

The peak at $t_R = 9.983$ min is isomannide, that at $t_R = 16.653$ min is 1,4-mannitan, while that at $t_R = 19.874$ min is the unreacted D-mannitol.

(b) Cycle 3, a, Fig. S12

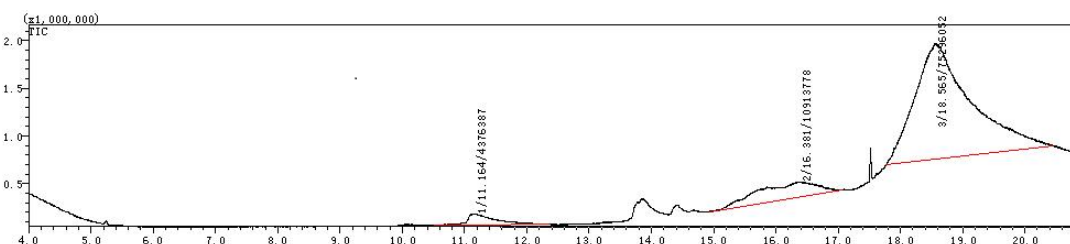


Fig. S66 GC part of GC-MS for Cycle 3, a, Fig. S12.

The peak at $t_R = 11.164$ min is isomannide, that at $t_R = 16.381$ min is 1,4-mannitan, while that at $t_R = 18.565$ min is the unreacted D-mannitol.

(c) Cycle 4, a, Fig. S12

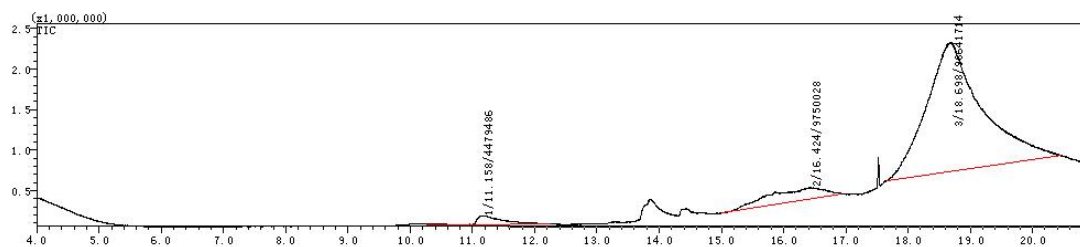


Fig. S67 GC part of GC-MS for Cycle 4, a, Fig. S12.

The peak at $t_R = 11.158$ min is isomannide, that at $t_R = 16.424$ min is 1,4-mannitan, while that at $t_R = 18.698$ min is the unreacted D-mannitol.

(d) Cycle 5, a, Fig. S12

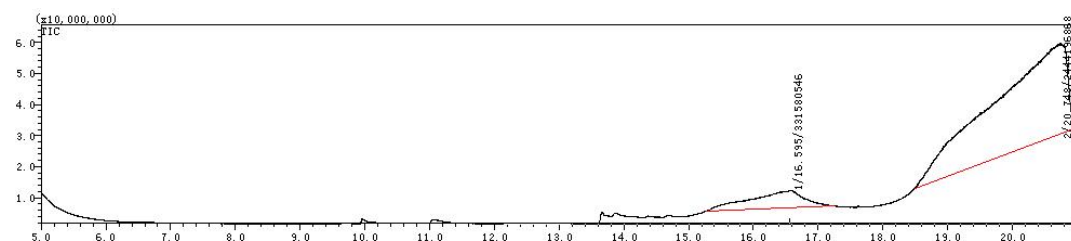


Fig. S68 GC part of GC-MS for Cycle 5, a, Fig. S12.

The peak at $t_R = 16.595$ min is 1,4-mannitan, while that at $t_R = 20.748$ min is the unreacted D-mannitol.

(e) Cycle 6, a, Fig. S12

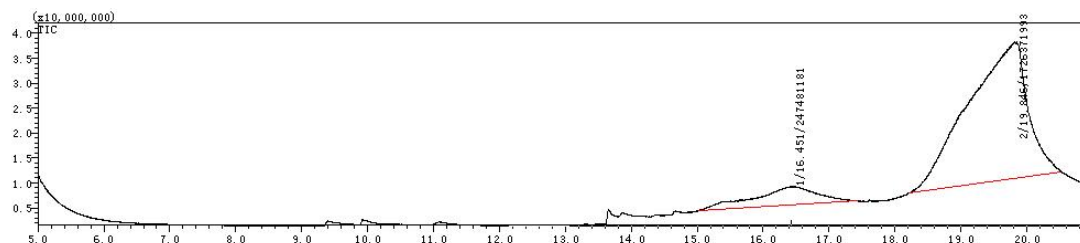


Fig. S69 GC part of GC-MS for Cycle 6, a, Fig. S12.

The peak at $t_R = 16.451$ min is 1,4-mannitan, while that at $t_R = 19.845$ min is the unreacted D-mannitol.

(f) Cycle 7, a, Fig. S12

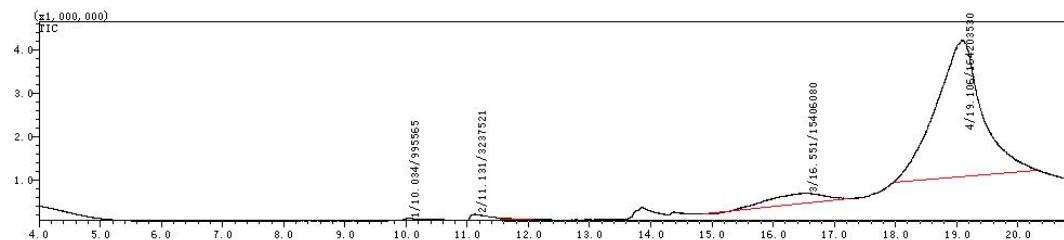


Fig. S70 GC part of GC-MS for Cycle 7, a, Fig. S12.

The peaks at $t_R = 10.034$ and 11.131 min is isomannide, that at $t_R = 16.551$ min is 1,4-mannitan, while that at $t_R = 19.106$ min is the unreacted D-mannitol.

Reference

[a] Shibata K, Kiyoura T, Kitagawa J, Sumiyoshi T, Tanabe K. Acidic properties of binary metal oxides. Bulletin of the Chemical Society of Japan, 1973, 46: 2985-2988